Report 5, 1993

RESERVOIR SIMULATION OF THE ALTO PEAK GEOTHERMAL FIELD, LEYTE, PHILIPPINES

Chona C. Bustamante,
UNU Geothermal Training Programme,
Orkustofnun - National Energy Authority,
Grensasvegur 9,
108 Reykjavik,
ICELAND

Permanent address:
Reservoir and Resource Management Department,
Geothermal Division,
PNOC-Energy Development Corporation,
Merritt Road, Fort Bonifacio,
Makati, Metro Manila,
PHILIPPINES

ABSTRACT

This study deals with the development of a numerical model for the Alto Peak geothermal field in Leyte, Philippines. Formation temperature and pressure profiles were estimated from heat-up surveys of five directional wells in this field. These profiles are indicative of an upflow zone beneath the New Alto Peak crater and an outflow to the south. The reservoir seems to be closed in the east. No conclusive data was gathered on the extent of the reservoir to the north and northwest. A three-dimensional grid of the reservoir was created to serve as input for the numerical simulator TOUGH. Several parameters of the TOUGH input were varied iteratively until a satisfactory match was reached between the measured and simulated temperatures and pressures of the wells. The steady state of the resulting best-fit model was able to replicate most of the prominent features of the observed temperatures and pressures. The current model, however, should be calibrated against production data before future predictions can be made.

TABLE OF CONTENTS

LIST OF FIGURES

LIST OF TABLES

1. INTRODUCTION

A geothermal reservoir model is a reservoir engineering tool that helps evaluate the geothermal resource and plan its development. It provides answers to a wide spectrum of reservoir management concerns such as well output decline, well spacing, reservoir potential, injection effects and potential subsidence. The first step towards this is the creation of a conceptual model. A conceptual model is a descriptive or qualitative representation of the current knowledge on the geosystem and its dynamics, and serves as a starting point for resource assessment. The process of making a conceptual model calls for an in-depth and thorough evaluation of the existing field data; analysis and integration of the reservoir data with the results of geological, geophysical and geochemical investigations; and an identification of the most significant physical processes that occur in the system. Based on the conceptual model, a mathematical or numerical model is created. The simulated reservoir behaviour using this model should be able to replicate the present reservoir responses and reliably predict its future performance.

Prior to exploitation, a field is considered to be in a quasisteady state due to the slow rate of change of the system's thermodynamic conditions (Bodvarsson et al., 1986). A quantitative model for this natural state, generally achieved through computer simulation, serves as a means to test and further refine the conceptual model. A successful natural state model will match quantitatively or qualitatively the salient characteristics and behaviour of the system, and thus, provide insights into important reservoir parameters such as formation permeability, boundary conditions for fluid and heat flow at depth, and the thermodynamic state of fluids throughout the system.

This report presents the results of the simulation study undertaken for the Alto Peak geothermal field in Leyte, Philippines. The first part of the report provides a general overview of the field under study. In the second part, a review of the existing knowledge of the field is presented, with emphasis on the results of geoscientific evaluations and the interpretation of these. The third part discusses the conceptual model which served as the basis for making the three-dimensional grid of the system. This 3D grid was used for simulating the natural state of the field using the TOUGH numerical code. TOUGH is an extremely powerful and complicated programme for simulating heat and fluid flow in a three-dimensional system. A considerable part of this study involved learning its capabilities and limitations.

2. THE ALTO PEAK GEOTHERMAL FIELD

2.1 Description and location

The Alto Peak geothermal field (Figure 1) is one of the eight geothermal areas distributed along Leyte Island, with Cabalian and Biliran as southern and northern boundaries, respectively. The field lies in Central Northern Leyte, approximately 8 km southeast of the Greater Tongonan Area. It is bounded by Mt. Mahanagdong in the northwest, Lake Danao in the southwest, Mt. Lobi in the south and East Leyte Plain on the east. The terrain is characterized by extremely rugged terrain with peaks ranging from 700-1310 m. It includes the volcanic complexes of Janagdan, Alto Peak and Cancajanag which are a part of the eastern range of the Leyte Cordillera.

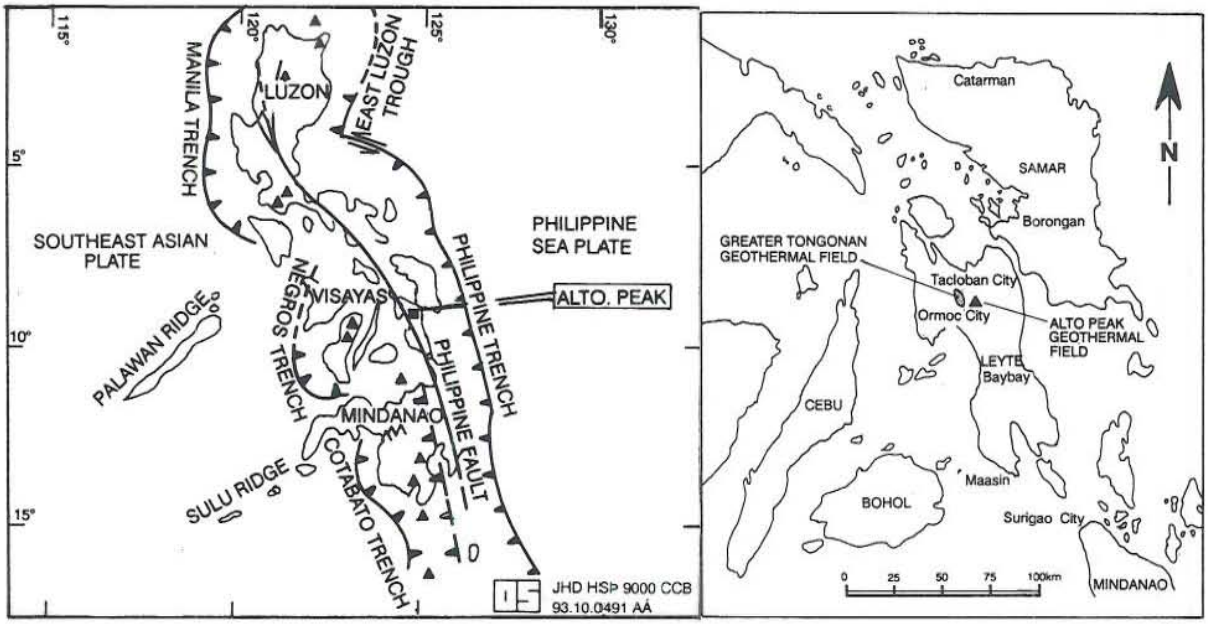

FIGURE 1: Location map of the Alto Peak geothermal field (mod. after Reyes et al., 1992)

2.2 Main geological features

The Alto Peak geothermal field lies along the traces of two major tectonic features; the Philippine Fault, a major left lateral strike slip fault which cuts across the Philippine arc from northwest Luzon to southwest Mindanao, and the East Philippine calc-alkaline volcanic front which extends from Bicol Peninsula in Luzon through Leyte Island and to Eastern Mindanao.

The southern segment of the Philippine Fault consists of a horst and graben system parallel to the main fault while the northern segment is deemed to be a pull-apart structure related to wrenching along the Philippine Fault. The western boundary of the pull-apart is a prominent feature while the eastern limit, though obscure, is believed to be controlling the alignment of the calc-alkaline volcanoes on the island (Reyes et al., 1992).

Volcanism of Alto Peak likely commenced in early Pliocene times, and persisted through the Pleistocene, as manifested by the majority of the rocks found on the surface. Effusive products of the different volcanic centers in the area are generally andesitic lava flows and pyroclastics, with associated domes and epiclastic deposits. The earlier deposits of Alto Peak were observed to be

intercalated with siltstones and calcisiltites, suggesting that the ancestral Alto Peak volcano was at least partially submerged in a marine environment during its active phase in the Pliocene epoch (Reyes et al., 1992).

2.3 Faults and structures

Three directional wells, AP-1D, AP-2D and AP-3D, were drilled in succession in 1991-1992 to generate an initial assessment of the proposed reservoir in Alto Peak. Two additional wells, AP-4D and AP-5D, were drilled during the second half of 1992. An integration of the basic well data for the five wells is summarized in Table 1.

TABLE 1: Basic well data of the Alto Peak wells
(Reyes et al., 1992; Salonga et al., 1993)

Well name	AP-1D	AP-2D	AP-3D	AP-4D	AP-5D
Elevation (m a.s.l.)	912	796	669	912	912
Wellhead coordinates	1227244 mN 470265 mE	1228406 mN 471188 mE	1227502 mN 472730 mE	1227268 mN 470275 mE	1227236 mN 470290 mE
Bottomhole coordinates	1226685 mN 471005 mE	1227511 mN 471366 mE	1226498 mN 472161 mE	1227098 mN 469057 mE	1226123 mN 470368 mE
Total depth	2012 mMD 1756 mVD	2502 mMD 2203 mVD	2723 mMD 2378 mVD	2644 mMD 2183 mVD	2423 mMD 2040 mVD
Throw azimuth (°)	111	163	210	263	176
Total throw (m)	802	913	1155	1225	1114
Kick-off point (m)	513	743	494	553	450
Casings (mVD)					
20"	100	100	97	102	99
13 3/8"	391	392	303	395	397
9 5/8"	944	1377	1372	967	913
Top of liner (mVD)	925	1345	1074	943	883
Bot. of liner (mVD)	1756	2188	2086	2183	2025
Spud-in date	27 June 91	11 Aug 92	12 Dec 91	16 July 92	07 Sept 92
Completion date	01 Aug 91	28 Oct 92	14 Apr 92	29 Aug 92	17 Oct 92

MD - measured depth, VD - vertical depth

AP-1D, AP-4D and AP-5D are located west of Danglog crater. AP-2D is situated north of the crater while AP-3D lies to the east. AP-1D, AP-2D and AP-3D were directed towards the crater area to intersect the postulated upflow zone. AP-4D and AP-5D were deviated to the west and south, respectively, to delineate the extent of the resource. Figure 2 shows a structural map of Alto Peak and the location of the wells.

During the well drilling and discharge phases, the northwest trending structures were generally associated with partial loss of circulation in all the wells; total loss of circulation occurred only in wells AP-4D and AP-5D when intersecting Tigbao Fault. For the northeast trending faults, only the Sulpa Fault intercepts in wells AP-1D and AP-5D caused partial loss of circulation. Similarly,

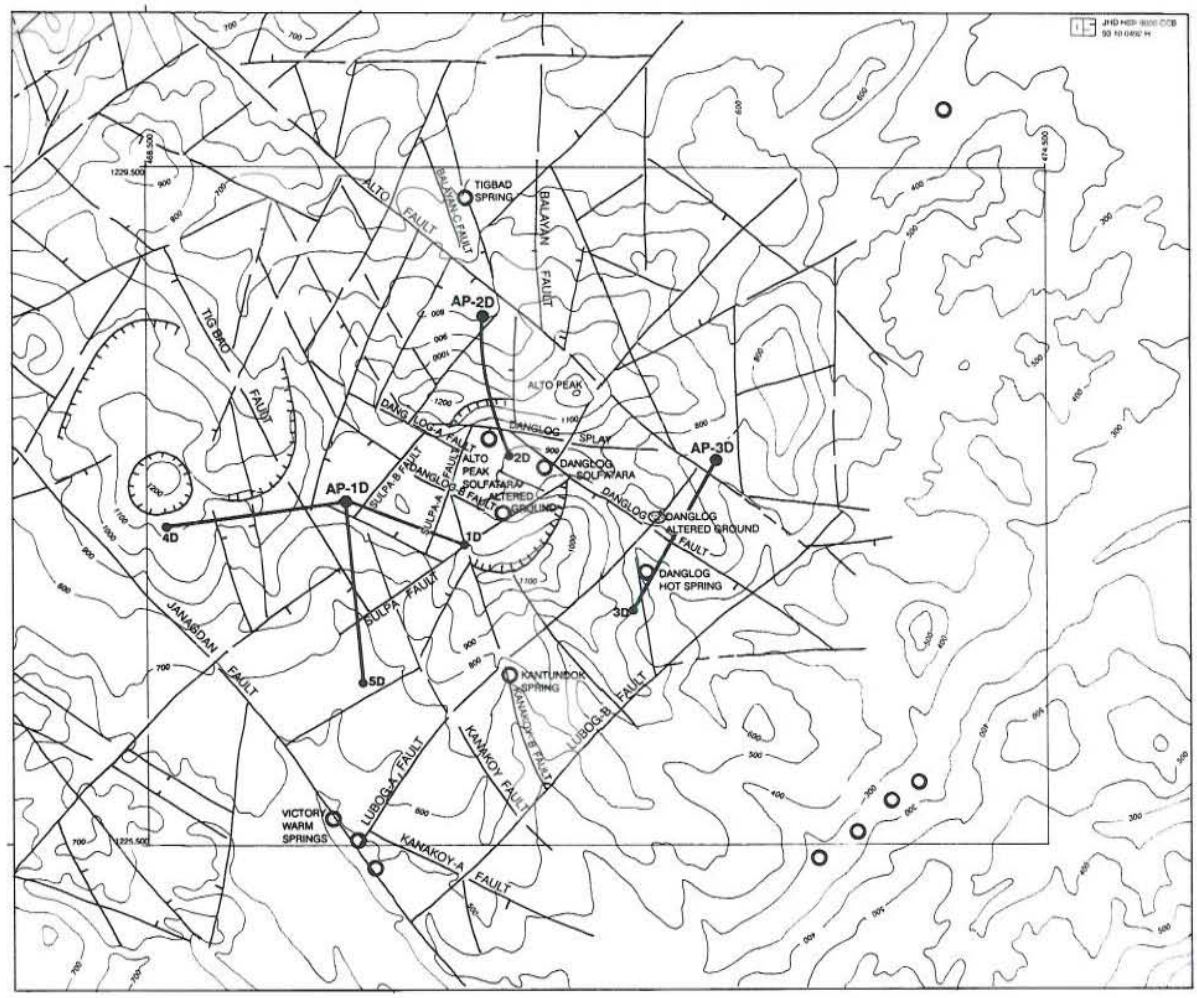

FIGURE 2: Structural map of the Alto Peak geothermal field (mod. after Reyes et al., 1992)

the east-west striking faults were identified with drilling losses and permeable zones while the north-south structures were merely associated with increased degree of alteration in the vicinity.

Analysis shows that structural permeability largely contributed to the flow among the wells (Salonga et al., 1993). The main channels for the hot fluids are Sulpa-A in AP-1D; and Danglog Splay, Balayan-C and Danglog Collapse Structure for AP-2D. The hot fluids seep westward towards Janagdan through these structures which all lie within the crater region. Cooler fluids, on the other hand, are predominantly in the south and east of the new Alto Peak crater. The conduits of the colder fluids are Sulpa for AP-1D and AP-5D; Kanakoy-B for AP-1D; Tigbao for AP-5D; and Danglog, Lubog-A and Alto for AP-3D. On the other hand, lithological permeability provides channels for horizontal migration of the fluids such as the shallow aquifer in AP-3D at 40-240 m where steam-heated waters from the crater region flow towards the Danglog springs in the east.

2.4 Geochemistry

The surface water samples collected from the area are generally secondary in nature; either they have been produced from the steam-heating of shallow groundwaters such as the Danglog and

Tapol springs, or by highly diluted near-neutral chloride springs such as the Victory and Binahaan springs. The narrow range in the Cl/B ratio (6-12) among the waters of Tapol, Mainit and Victory springs is indicative of the homogeneity of the parent fluid. Moreover, the similarity in the Cl/B ratio between the waters from wells AP-1D, AP-2D and AP-5D and the waters of the Tapol and Victory springs shows the affinity of the surface springs to the well fluids. This would suggest that these springs are indeed outflows from the deeper reservoir fluid (Salonga et al., 1993).

2.5 Geophysical survey

The resistivity map of Alto Peak is shown in Figure 3. As can be seen in the figure, the central region of Alto Peak is characterized by an anomaly of less than 10 Ωm. This low resistivity anomaly may be due to one or more of the following: high porosity, high permeability, high temperature, high salinity or increased alteration. On this basis, this study concentrated on an area enclosing the resistivity anomaly.

Furthermore, the boundary in the north appears to be slightly depressed to the south. A 20 Ωm lobe to the northeast may be related to a minor outflow towards the Mainit warm spring where resistivities decrease with depth.

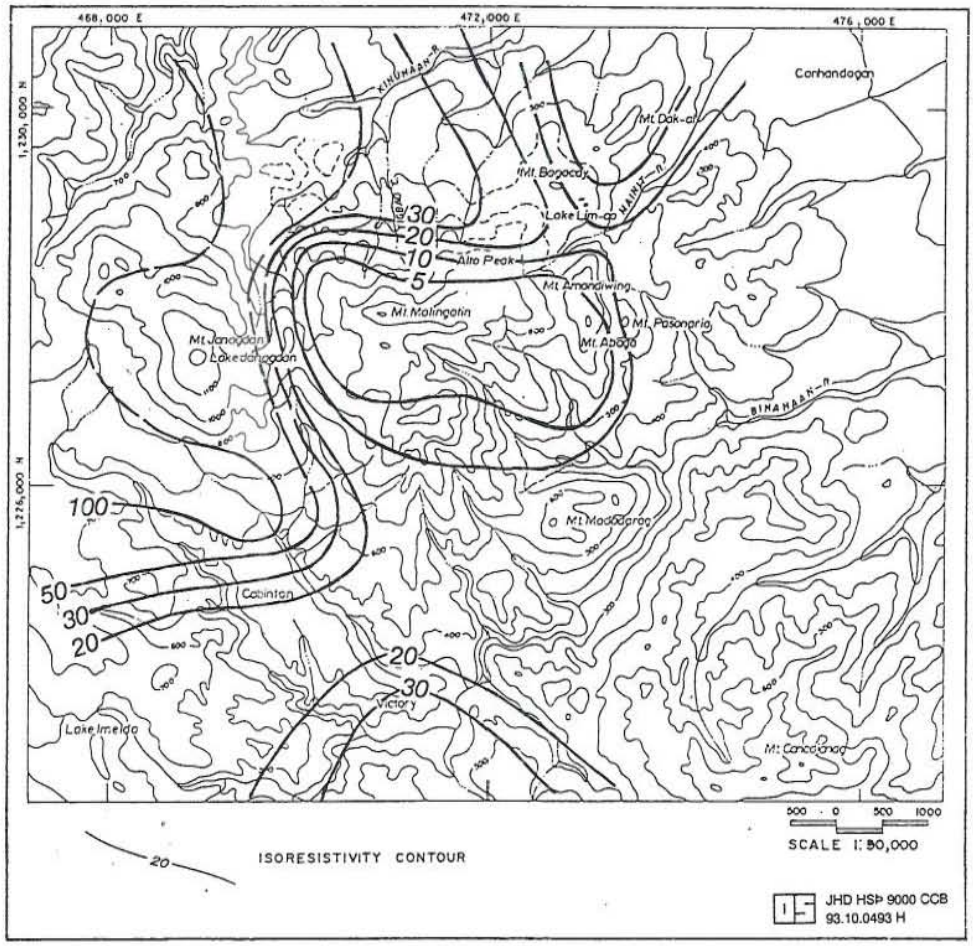

FIGURE 3: Isoresistivity map of the interpreted Alto Peak subsurface, values in Ωm (Salonga et al., 1993)

3. WELL ANALYSIS

In characterizing a geothermal reservoir and assessing its potential, a large volume of data is analyzed to obtain representative values for the hydrological and thermal properties of the fractured rock mass. These data are products of the completion tests, heat-up surveys and bore output measurements that were conducted on the wells in the field. The completion tests consist mainly of waterloss surveys that help identify the well's permeable zones; and pressure transient tests, such as an injectivity index and a pressure fall-off test, that give an estimate of the overall permeability of the formation around the well. These tests are generally conducted for days so that they are a good indication of the flow properties of the fractures. The highlights of the results of the completion tests and the bore output measurements are summarized in Table 2.

TABLE 2: Well test summary (Salonga et al., 1993)

	AP-1D	AP-2D	AP-3D	AP-4D	AP-5D
Perm. zones (mVD)					
major	1380-1430	1820-1900	1850-1900	1465-1625	1950-2030
minor	1530-1550	2150-2200	2050-2100	1940-2083	866-1060
	1700-1750	1630-1670			1217-1255
					1330-1410
Water level (m) *	150	300	400	200	300
Injectivity (l/s-MPa-g)	27.5	275	14.5 w/very high WHPs	23 w/WHP 0-1.31 MPag	14-19
Permeability-thickness product (Dm)	12-13	very high	0.64	0.64-1.3	2.6-9.2
Max. temp/location (°C/mVD)	309/1385	345/2200	186/2070	243/1424	268/1178
Initial output (FBD)					
MF (kg/s)	5	120-130	0	12.5	9.0
H (kJ/kg)	2100	1600-1700	-	1140	990
WHP (MPag)	1.65	1.5	-	0.25-0.40	1.05

* Below casing head flange, extrapolated to zero pressure level,
WHP - wellhead pressure, FBD - full bore discharge
MF - mass flow, H - enthalpy,

The injectivity test is performed by measuring the downhole pressure of a specific point in the borehole, usually within the vicinity of the main permeable zone if not exactly across it. The result of this test is the injectivity index, expressed in l/s-MPag, which is a measure of the well's capacity to accept the water injected into it. On the other hand, the pressure fall-off test is performed by measuring the change in pressure in the well at specified time intervals at zero water flow. From the data, the permeability-thickness product (kh), which is expressed in darcy-meter (Dm), can be calculated.

The heat-up surveys are done after shutting the well which has just undergone the completion tests. The resulting profiles help confirm the existence of the permeable zones earlier identified through waterloss surveys. Moreover, they manifest the rate of temperature and pressure recovery of the well after the massive influx of water it experienced during drilling and the conduct of the

completion tests. Generally, a fast thermal recovery signifies high permeability.

On the other hand, the bore output measurements provide an initial estimate of the output of the well, and a gauge of its capacity to sustain commercial wellhead pressure through the use of back pressure plates. Back pressure plates constrict the fluid path and induce production from less active permeable zones.

3.1 Well permeability

1AP-2D proved to be a very permeable well, as reflected by the high injectivity index of 275 l/s-MPag. The pressure transient tests also confirmed this qualitatively through very small pressure changes during the injection of more fluid. Consequently, no value for the permeability-thickness product was computed. AP-1D likewise exhibited average to good permeability, although lower than AP-2D, with an injectivity index of 27 l/s-MPag and a permeability-thickness product of 12-13 darcy-meters at zero or vacuum wellhead pressure during the pressure transient tests.

The three other wells (AP-3D, AP-4D and AP-5D) exhibited poor permeabilities with AP-3D proving to be the least permeable. AP-3D is characterized by low temperature and very poor permeability (kh = 0.64 Dm). Very high wellhead pressure was encountered during water injection. AP-4D likewise experienced high wellhead pressure during the completion tests thus, indicating poor permeability. The injectivity index is low at 23 l/s-MPag considering high wellhead pressure during the conduct of the test. The permeability (kh = 0.64-1.3 Dm) is very much lower than that of nearby AP-1D. AP-5D also showed low permeability with an injectivity index of 14-19 l/s-MPag and kh of 2.6-9.2 Dm.

3.2 Stable formation temperatures and pressures

Although the wellbore was highly quenched with drilling fluids, its heat-up temperature and pressure profiles helped estimate the stable formation temperatures and pressures of the wells. Generally, though, a lowering of the temperature at the upper zones was done to downplay the effect of steam influx from the lower zones. This modification, however, is corroborated by geoscientific findings such as alteration mineralogy and fluid inclusion data.

The software BERGHITI was used to approximate the stable formation temperatures at different elevations. It utilizes the Horner method in a plot of T vs. ln $(\Delta t/(\Delta t + t_c))$. Figures 4-8 show the measured temperature and pressure profiles for each of the five wells.

The estimated stable formation temperature profile derived using BERGHITI and geoscientific evaluation is represented by a continuous dark line (Figures 4-8). The five estimated stable formation temperature profiles are plotted together (Figure 9). A detailed look at the heat-up pressure profiles revealed the pivot point for the wells. The pivot point refers to a particular depth where the pressure is stable throughout the conduct of the heat-up surveys; hence, it is believed to represent the true reservoir pressure. The pivot point was used for calculating the stable pressure profiles using the software PREDYP. An integrated plot of the estimated stable formation pressure profiles for the five wells is shown in Figure 10.

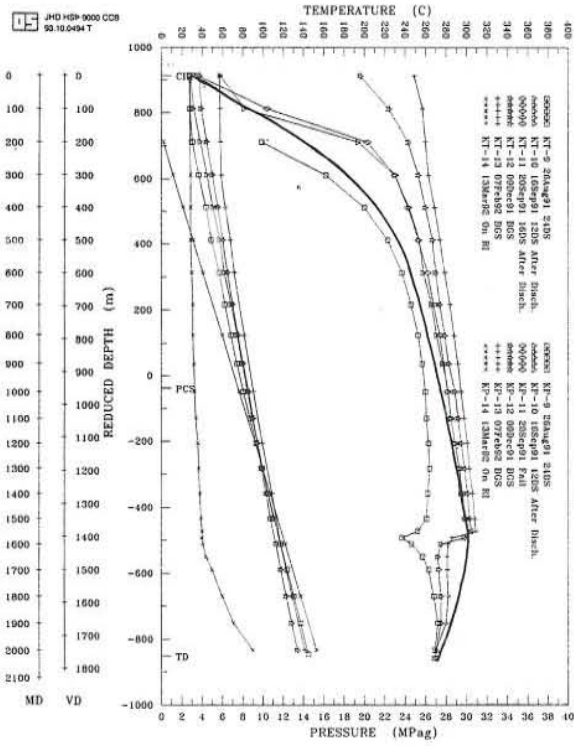

FIGURE 4: AP-1D measured temperature and pressure profiles

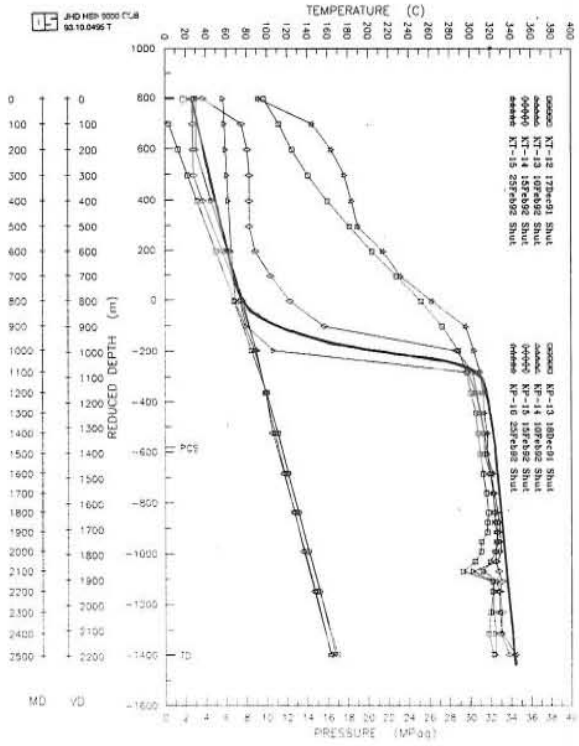

FIGURE 5: AP-2D measured temperature and pressure profiles

3.2.1 AP-1D

The major feed zone in this well was identified to be at 1380-1430 mVD through the heat-up profiles of the well (Figure 4). A rapid build-up of temperature at this depth suggests a two-phase inflow. This inflow was gas-rich as shown by the sudden increase of wellhead pressure to 6.9 MPag in just two days after the completion tests even if the well was on bleed. Below this depth is a persistent temperature inversion. The well's temperature is high; the maximum temperature measured in AP-1D is 309°C at 1389 mVD. The estimated stable formation temperature profile of AP-1D is similar to the heat-up profiles. The temperature at the upper layer was deemed to be lower than what is reflected in the heat-up surveys because in these profiles, the presence of steam in the borehole must have already raised the temperature in the upper zone.

The pivot point is located at -460 m a.m.s.l. at a pressure of 11.0 MPaa. Using PREDYP, the stable formation pressure profile is shown in Figure 10.

3.2.2 AP-2D

The plot of the heat-up profiles of AP-2D (Figure 5) shows the well's rapid temperature recovery from the massive quantity of cold water injected into it during the completion tests. After only one day of shut condition, the temperature already reached 290°C. The maximum recorded temperature in the well is 345°C at 2200 mVD.

It is apparent that the upper zone (0 to 900 mVD) is cold with temperature less than 100°C. Fluid inclusion and alteration mineralogy findings agree with these results. The estimated stable

formation temperature profile followed closely the profiles of the early heat-up surveys. The pivot point is located at -320 m a.m.s.l. at a pressure of 9.80 MPaa (Figure 10).

3.2.3 AP-3D

Low temperature characterizes the well. The maximum temperature after 24 days of shut-in is a mere 186°C at the bottom. The heat-up rate is slow and steady. The estimated stable formation temperature profile (Figure 6) followed closely the heat-up profiles.
The pivot point is at -150 m a.m.s.l. at a pressure of 4.0 MPaa (Figure 10).

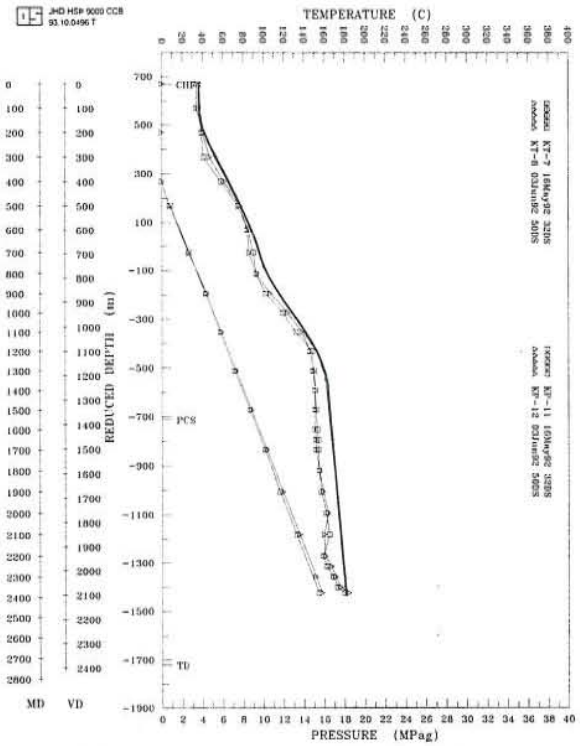

FIGURE 6: AP-3D measured temperature and pressure profiles

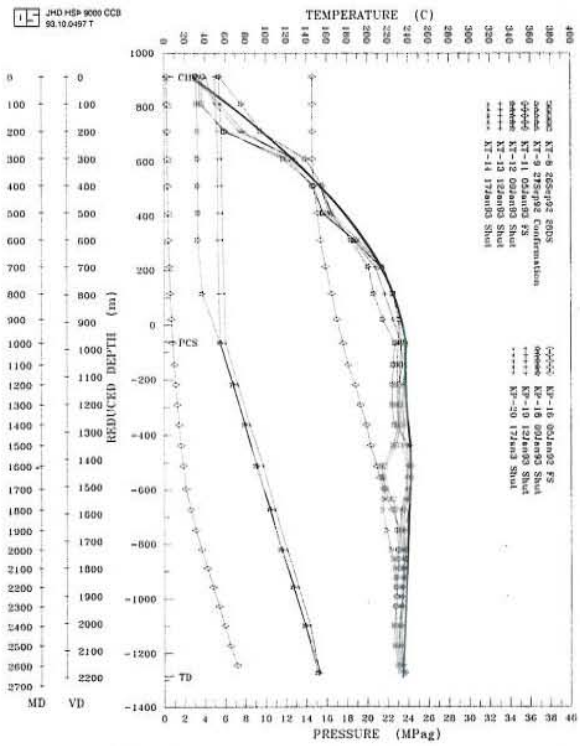

FIGURE 7: AP-4D measured temperature and pressure profiles

3.2.4 AP-4D

AP-4D steadily increased its temperature during the heat-up surveys. No wellhead pressure developed throughout the heat-up period. The major loss zone is located at 1465-1625 mVD. No pivot point was deduced from the heat up profiles. Apparently, like AP-1D, there is a temperature inversion in the lower zone. Like the first three wells, the estimated stable formation temperature profile (Figure 7) followed closely the early heat-up surveys' profiles, and the temperatures in the upper layer were deemed actually lower than those reflected in the early heat-up surveys.

3.2.5 AP-5D

The heat-up profiles (Figure 8) show a steady temperature build-up with time. The upper zone of the well indicates two phase vapour/gas conditions. The high wellhead pressure developed by the well supports the existence of these 2-phase fluids above the production casing shoe in AP-5D. Like AP-1D and AP-4D, temperature inversion is evident at the bottom. The pivot point is

located at 200 m a.m.s.l. with a pressure value of 4.5 MPaa.

The estimated stable formation temperature profile was largely based on the heat-up profiles like the rest of the wells. The inversion is also apparent in the bottom zones like AP-1D and AP-4D.

3.3 Bore output measurements

Reserve estimate studies and Monte Carlo simulations of the field show that it has a potential of 80 MW_e (Salonga et al., 1993). AP-2D is considered as the prime resource of the field because it proved to have the greatest capacity among the five wells with an output of about 20 MW_e. AP-1D, AP-4D and AP-5D are all marginal wells in terms of output. AP-3D did not discharge. This was not surprising because earlier in the completion tests and heat-up surveys, it already exhibited low temperature and permeability. The initial discharge data for the wells is shown in Table 2.

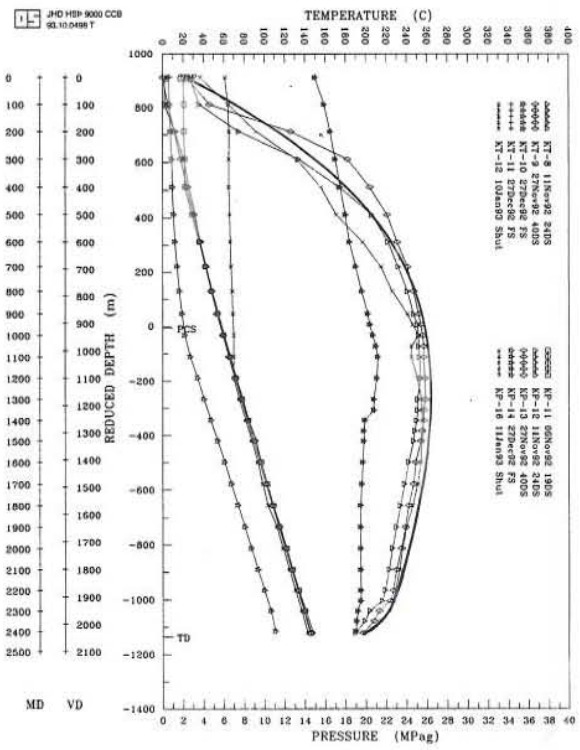

FIGURE 8: AP-5D measured temperature and pressure profiles

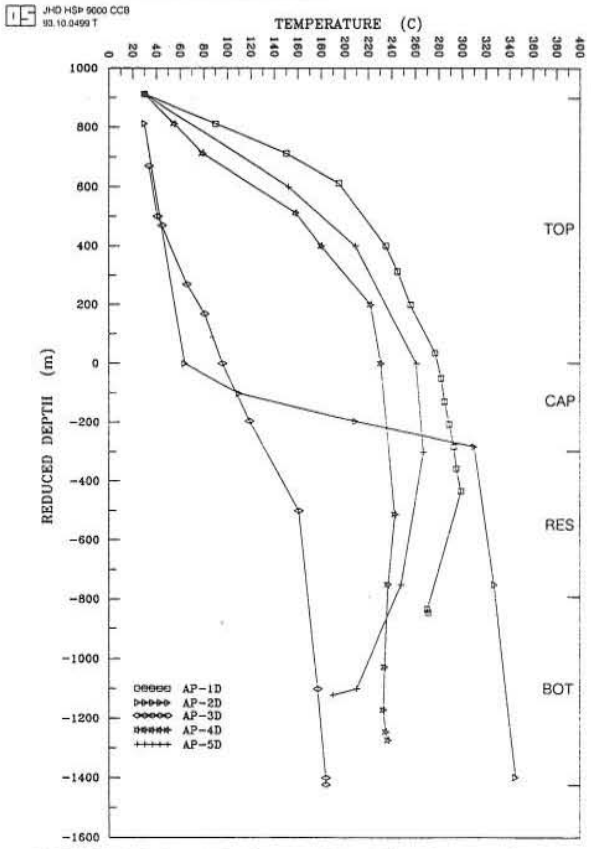

FIGURE 9: Estimated stable formation temperature profiles for the five wells

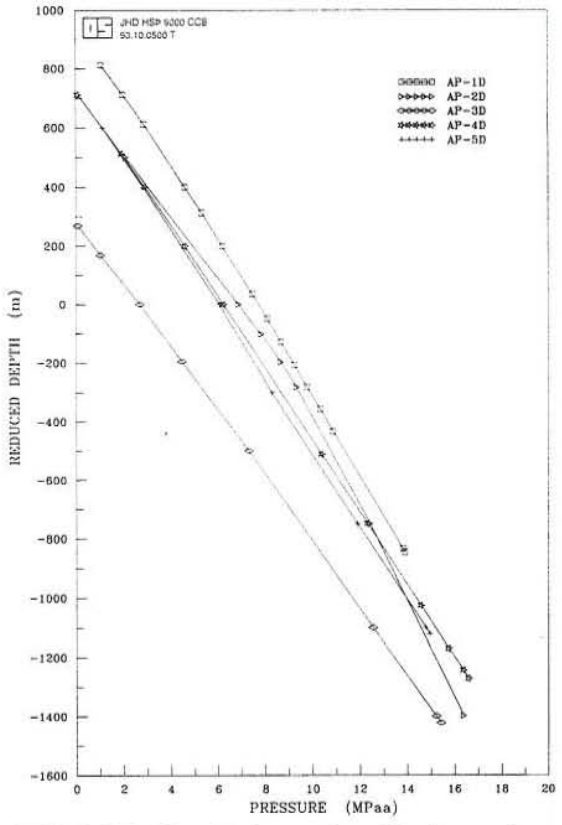

FIGURE 10: Estimated stable formation pressure profiles for the five wells

4. CONCEPTUAL MODEL

4.1 Temperature and pressure contours

Temperature and pressure contours were created for several elevation depths. Figure 11 shows the temperature contour at -550 m a.m.s.l.. This map is representative of the other depths (+650 +200, -150, and -1100 m a.m.s.l.). The AP-3D side, is believed to be in a cold block. The temperatures and pressures in the east are low. Based on the contours, the temperature and pressure are highest in the area between AP-1D and AP-2D. However, the contour lines north of AP-2D are uncertain because this area has not yet been delineated.

The contours in the south reveal low temperature and pressure. The water from the upflow zone close to AP-2D most likely takes the path towards this sector. This is validated by the temperature inversions observed in the lower zones of AP-1D, AP-4D and AP-5D.

4.2 Hydrological model

The hydrological model of the field is shown in Figure 11. Water flows through channels from AP-2D in the north towards the outflow at the south where AP-1D, AP-4D and AP-5D are located.

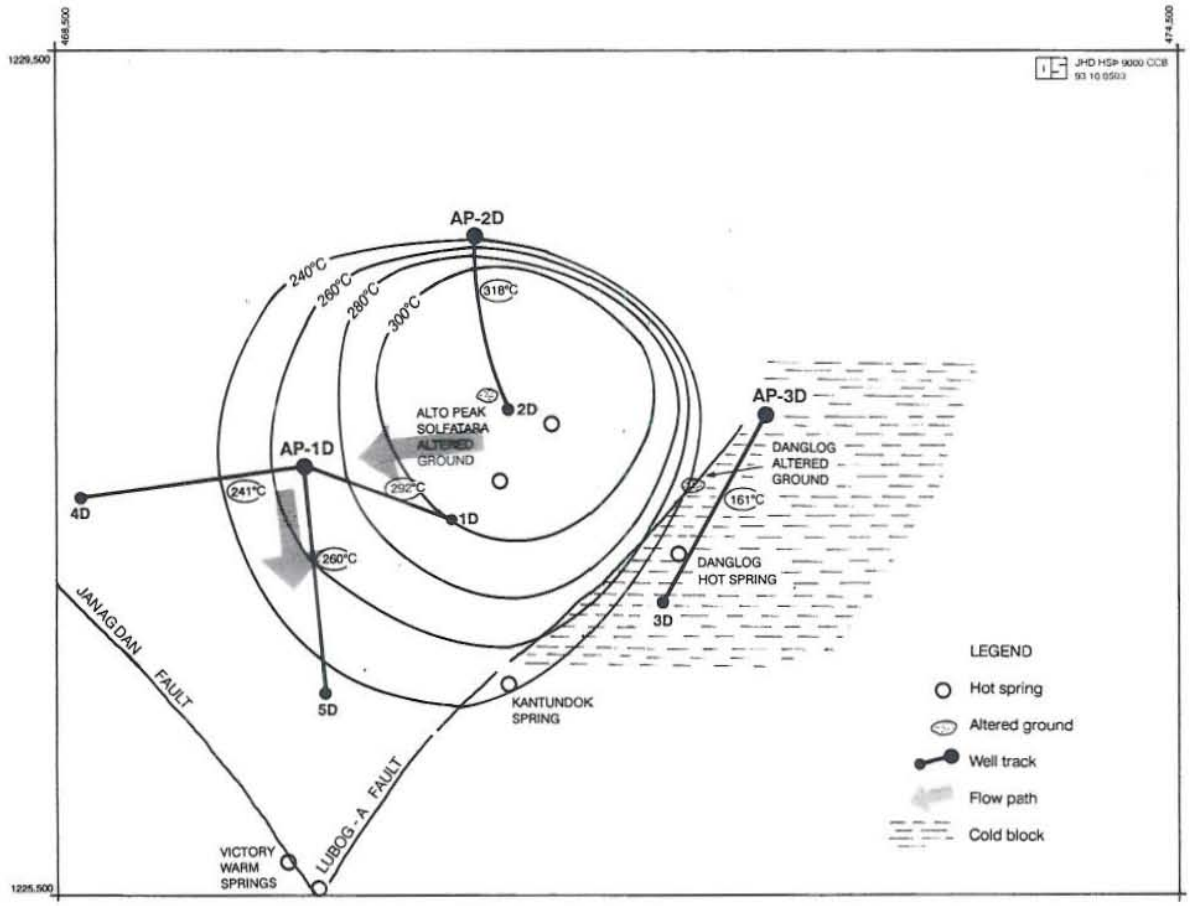

FIGURE 11: Hydrological model of the Alto Peak geothermal field

The upflow is situated beneath the New Alto Peak crater where solfatara, altered grounds and mudpools abound. This agrees with the results of the well testing phase that AP-1D and AP-2D have high temperatures. The bottomhole temperatures of these two wells range from 280 to 345°C. The presence of actinolite and secondary biotite were likewise noted. AP-2D, may be cold at shallow depths, but it actually penetrated the hottest sector of the field where several dyke intrusions occur. Nothing much, though, can be said of the area further north of AP-2D because it has remained unexplored. Nonetheless, the existence of a steep resistivity gradient (Figure 3) between the hot central region and the north and northwest areas suggests decline in temperature towards the north and the northwest.

Well AP-3D, drilled outside the crater region, showed subsurface temperatures of not more than 200°C down to 1709 mVD, thus, proving the existence of a cold block in the eastern side of Alto Peak. This is supported by geological findings that showed the occurrence of smectite, opal goethite and low temperature zeolites down to the bottom of the well. The Lubog-A Fault most likely channels the hot fluids towards the nearby hot springs and even to the Victory warm springs, instead of to the east in the direction of AP-3D.

The outflow most likely lies in the south where AP-1D, AP-4D and AP-5D are situated. The lateral stream of thermal fluids moving towards the south possibly supplies the thermal waters to the outlying springs of Victory and Kantundok. These three wells encountered thermal inversion in the lower zones. AP-4D and AP-5D encountered hot (250-260°C) fluids at shallow depths, but experienced temperature reversals at deeper levels. The degree of inversion, however, is more pronounced in AP-5D than in AP-4D. This is consistent with the alteration mineralogy and fluid inclusion results which predicted a bottomhole temperature of 240°C in AP-4D (1270 mVD) but only 200°C in AP-5D (1130 mVD). Temperature surveys show that in the vicinity of AP-4D, which is the area covered by Mt. Janagdan, higher temperature is encountered at deeper levels compared to AP-3D and AP-5D. Furthermore, AP-4D shows gradually declining temperature to the west, thus limiting the productive resource extension towards Mt. Janagdan.

5. NATURAL STATE SIMULATION

5.1 Objectives and methodology

Modelling the pre-exploitation conditions of a geothermal field or natural state simulation, is desirable prior to exploitation modelling because it helps verify the validity of the conceptual model and quantify the natural mass flow within the system. It likewise provides the necessary initial thermodynamic conditions for exploitation modelling.

Natural state simulation involves the setting up of a model with an approximate permeability structure based on the conceptual model. The model should include enough volume to encompass the convective system purportedly existing and the block structure of the model should be simple to begin with (O'Sullivan and McKibbin, 1989).

A numerical grid of the entire system or its subset is used during the computer simulation runs to match the observed thermodynamic field conditions such as temperature and pressure distributions. The simulation of the model should be carried out over a very long period of time corresponding to the development of the system over geological time. The resulting steady state or natural state simulations should have the following features approximately correct:

a. Temperature distribution
b. Location and magnitude of surface features, both mass and heat flows
c. Correct pressures (boiling point with depth in two-phase zones).

Iterations are made by changing the permeability distribution of the system and the strength of the mass and heat upflow into the system until the calculated results match the observed data. Since the natural-state model is calibrated against the observed three-dimensional temperature and pressure distribution, it is very important to get accurate measurements during pressure and temperature surveys. Moreover, many iterations are often required with the adjustment of the permeability structure (Bodvarsson and Witherspoon, 1989). To match these features accurately, the model must have the large-scale permeability structure approximately correct. This is the determining factor of the long-term behaviour of the system under exploitation.

In this study, the software TOUGH was used in the natural state simulation of the Alto Peak geothermal field. TOUGH is a numerical simulator used for modelling the coupled transport of water, vapour, air and heat in porous and fractured media (Pruess, 1987). It is a member of the MULKOM family of multi-phase, multi-component codes, which is being developed at Lawrence Berkeley Laboratory primarily for geothermal reservoir applications. The acronym "TOUGH" stands for "transport of unsaturated groundwater and heat." TOUGH has so far been applied mostly to studies of high-level nuclear waste isolation in partially saturated geological media. However, it has been utilized also for a wider range of problems in heat and moisture transfer, and in the drying of porous materials.

5.2 The three-dimensional grid

Figure 12 shows the grid that was used for the natural state simulation. It has an area of 24 km^2 within the confines of the coordinates 468,500 to 474,500 mE and 1,225,500 to 1,229,500 mN. The area was subdivided into 43 blocks. The centre of each block or the coordinates of a well, in the presence of one, represents the whole block. The five well tracks were partitioned into several layers deemed most representative of the conditions at particular elevations, largely based on the estimated stable formation temperature plot of the five wells (Figure 9).

The layers in the grid are as follows: TOP, CAP, RES, BOT, BAS and SUR. Both the BAS and SUR layers were assigned very big volumes (1.0 x 10^{20} m^3) and very low permeabilities of 0.1 x 10^{-20} m^2. The height of the blocks in the TOP layer was made variable to follow the natural elevation of the area.

Three programmes helped reduce the tedious process of creating the TOUGH input file. These are ELEME_SCALE, CONNE_SCALE and CONNE_LAYER, all by Pordur Arason at Orkustofnun.

The TOUGH output file is usually very large (1-2 Mbytes) so, three programmes; AWK-TOUGHE, AWKTOUGHF, AWKTOUGHT by Tomas Johannesson, likewise of Orkustofnun, were used extensively to extract relevant information for various graphs. Moreover, the programme SP by Einar Kjartansson and Tomas Johannesson was used to draw XY graphs, and the programme CONTOUR by Pordur Arason and Grimur Bjornsson to draw contour graphs.

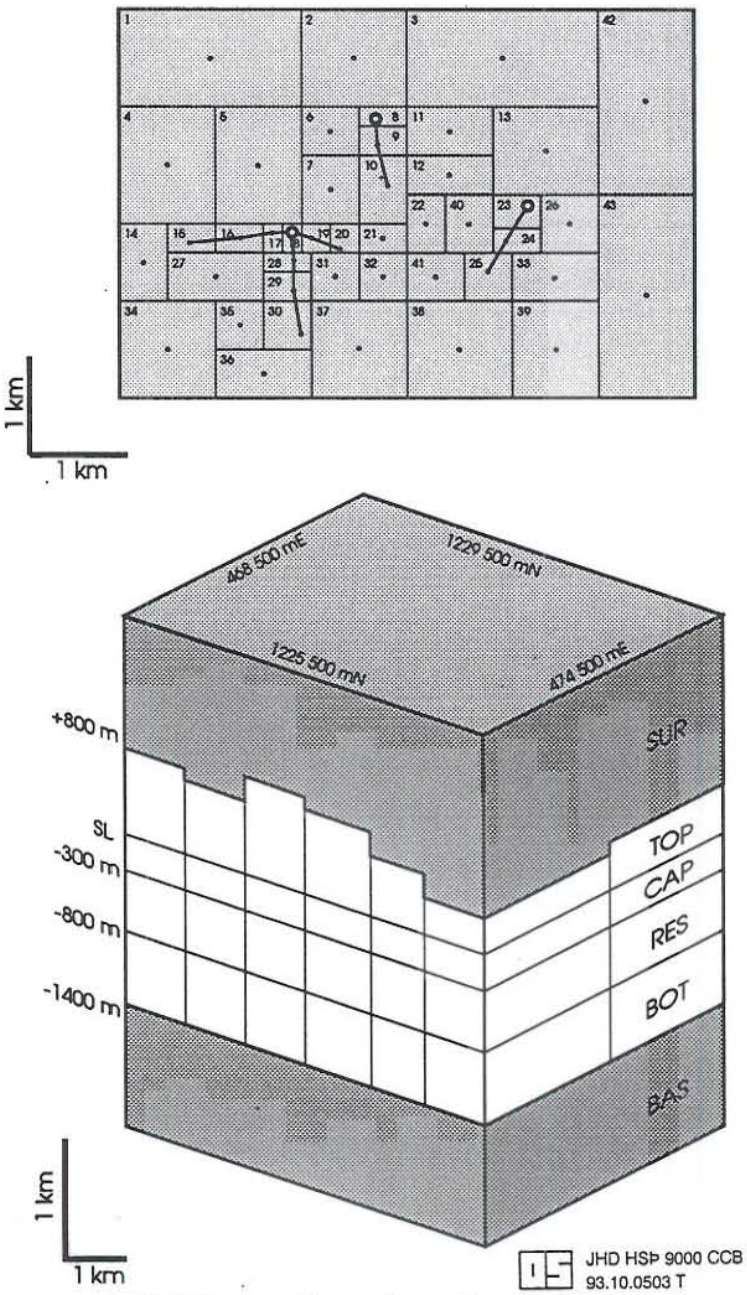

FIGURE 12: Three-dimensional grid of the Alto Peak geothermal field

BOT 10 and 21 served as the recharge blocks in the model, each at a mass flow rate of +5 kg/s and an enthalpy of 1800 kJ/kg. The constant pressure and constant temperature blocks SSI in the south and ESI in the east of the CAP layer were used as sinks for the fluids in the system and the resulting excess fluids due to heat-up expansion. Block SSI is connected to CAP 34, CAP 36, CAP 37 and CAP 38 while block ESI is attached to CAP 42 and CAP 43. Blocks SSI and ESI both have very high permeability (1000 mD), high specific heat (10^6 J/kg-°C), and very large volume (10^{20} m^3).

5.3 Results of the natural state simulation

Several parameters in the TOUGH input file were varied iteratively until a satisfactory match was found between the observed and simulated temperatures and pressures of the wells. Figures 13 and 14 show how the temperature and pressure of element RES 24 have already stabilized through the TOUGH run for the best fit model, thus, validating the results. RES 24 was chosen for monitoring because it is far from the source; it is believed that by the time it stabilizes, all the rest have already stabilized.

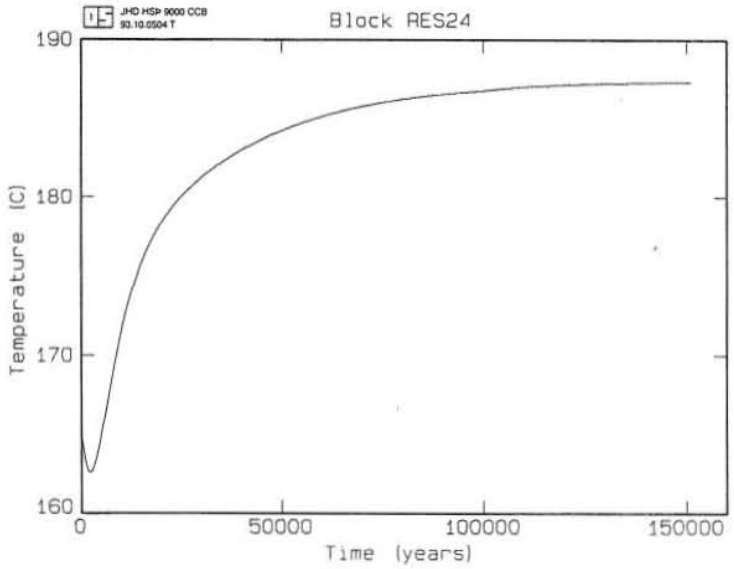

FIGURE 13: Stabilization of temperature in element RES 24 vs. time

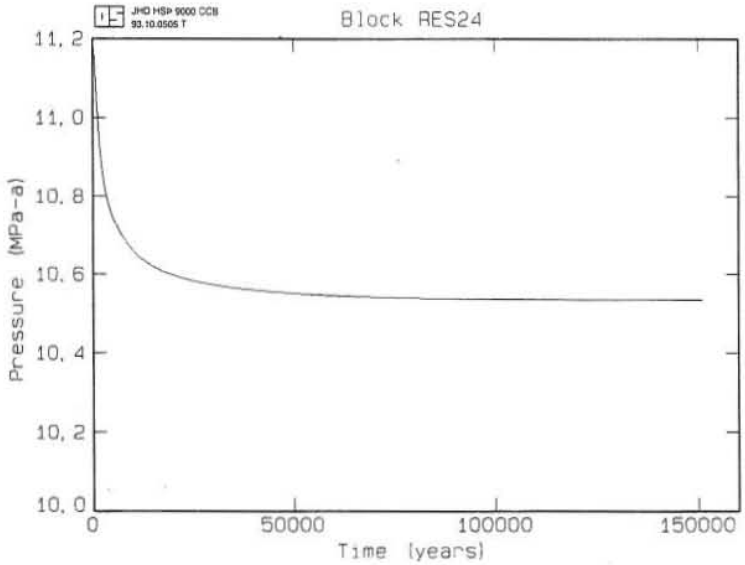

FIGURE 14: Stabilization of pressure in element RES 24 vs. time

Figure 15 shows the match between the estimated stable formation temperatures and the TOUGH-simulated temperature data. The simulated data points were able to duplicate the thermal inversion at the bottom zones of AP-1D, AP-4D and AP-5D. The trend for the simulated data points for AP-3D is similar to the estimated stable formation temperature profile. In the case of AP-2D, the temperature of the simulated data point for the TOP layer is much higher than what is reflected in the stable formation temperature profile. This is believed to be due to the presence of cold shallow groundwater and an impermeable caprock sitting atop the RES layer. However, this complication was not incorporated into the model and therefore, there is a significant mismatch between the observed and simulated temperatures in AP-2D.

The match between the estimated stable formation pressures and the TOUGH-simulated pressure data is shown in Figure 16. All the wells, except AP-3D, show an acceptable match. The simulation was unable to reproduce the very low pressures observed in well AP-3D. In fact, it can be stated that if the estimated formation pressures in AP-3D are correct, then the blocks in the AP-3D side are not hydrologically connected to the reservoir. It is quite possible that the Lubog-A Fault is separating AP-3D from the reservoir.

Figure 17 shows the permeability distribution of the best-fit computer simulation run. Permeabilities varied from 0.1 to 50 mD. In the BOT layer, elements BOT 10 and BOT 21, being the sources, have the highest permeability (50 mD). The permeability of the blocks around AP-1D, AP-4D and AP-5D have permeabilities of 20 mD. The blocks surrounding them have low permeability at 0.5 mD.

Twelve rock types were used in the best-fit model. A rock density of 2700 kg/m^3 was assigned to all the rock types. A thermal conductivity value of 1.5 W/m°C was likewise uniformly assigned to them. Apart from elements controlling the boundary conditions, the specific heat of the rocks was uniformly set to 1 kJ/kg°C. Table 3 summarizes all the rock properties used in the best fit model.

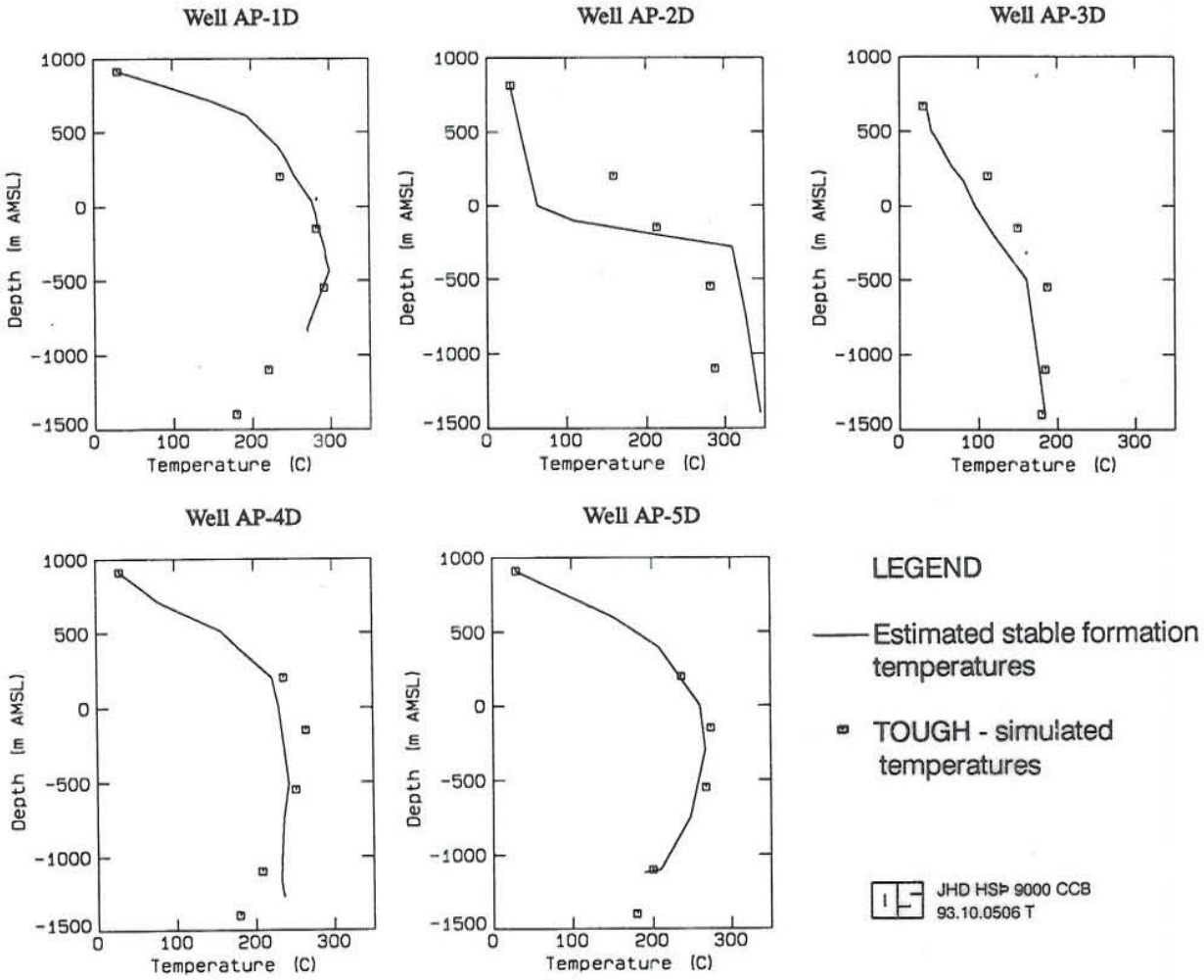

FIGURE 15: Estimated stable formation temperatures vs. TOUGH simulated temperatures

TABLE 3: Rock properties of the best-fit model

Rock type	Density (kg/m^3)	Porosity (%)	Permeability (mD)	Thermal conduct. (W/m°C)	Specific heat (J/kg°C)
topr1	2700	5	0.5	1.5	1000
topr3	2700	5	0.1	1.5	1000
capr1	2700	5	5.0	1.5	1000
capr3	2700	5	0.1	1.5	1000
resv1	2700	8	5.0	1.5	1000
resv2	2700	8	20.0	1.5	1000
resv3	2700	8	0.5	1.5	1000
botm1	2700	8	20.0	1.5	1000
botm2	2700	8	50.0	1.5	1000
botm3	2700	8	0.5	1.5	1000
cons1	2700	10	1000	1.5	1000000
cons2	2700	0.	0.1	1.5	1000000

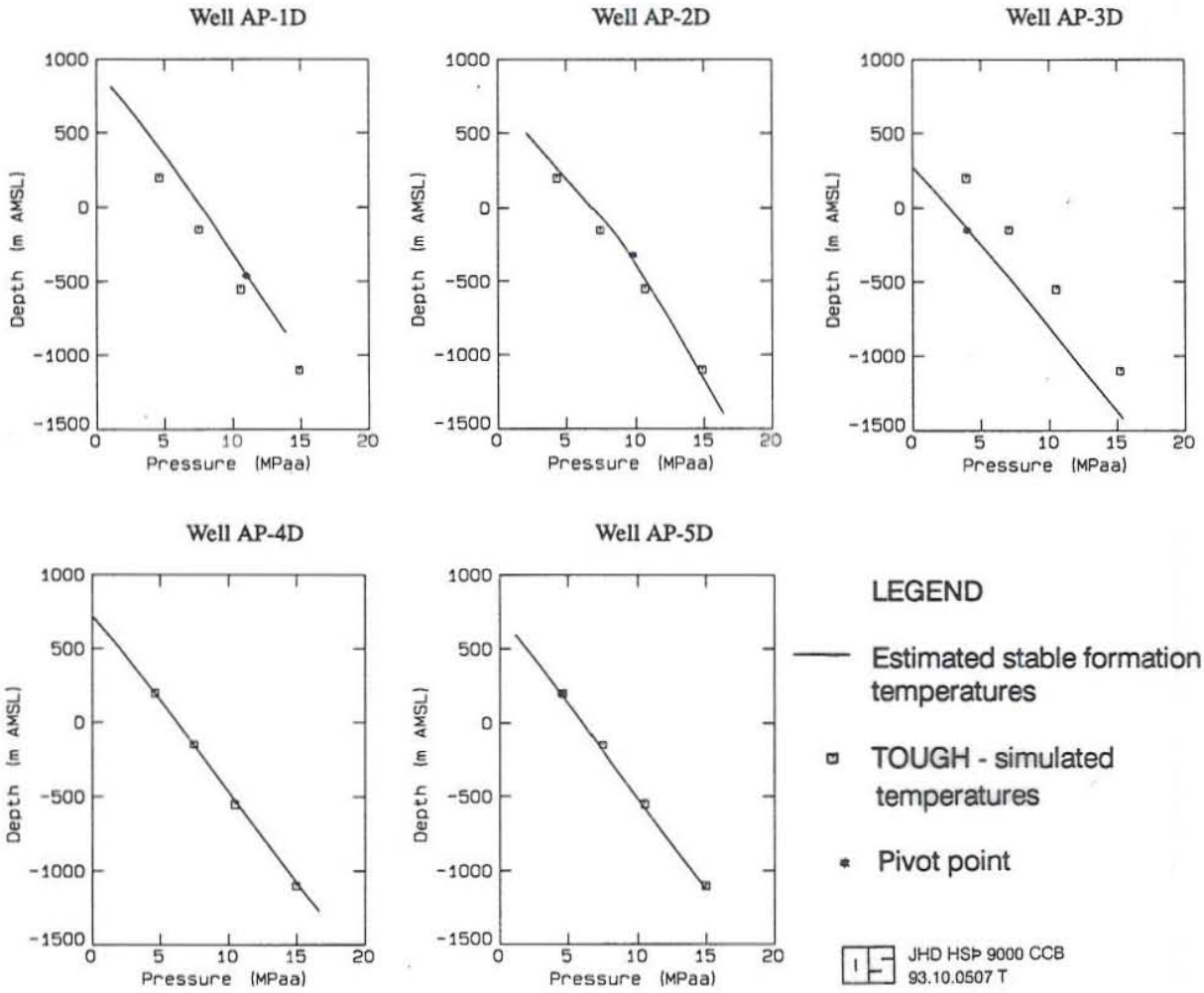

FIGURE 16: Estimated stable formation pressures vs. TOUGH simulated pressures

The permeability distribution in the RES layer is similar to the BOT layer; RES 11, RES 12 and RES 22, however, were not assigned the highest permeability value (20 mD) in that layer, unlike in the BOT layer. This was done to avoid flow into these blocks, and instead, direct the flow towards AP-1D, AP-4D and AP-5D to heat them up. In the CAP layer, the blocks within the vicinity of AP-1D, AP-4D and AP-5D were assigned a high permeability (5 mD) and the remaining blocks were assigned a low permeability of 0.1 mD to direct the flow towards the sink in the south. Furthermore, the horizontal connections among blocks 37, 40 and 41 were given slightly higher permeabilities (sort of anisotropy) to approximate the Lubog-A Fault's role in the field.

The temperature and pressure contours that were derived from the best fit simulation run are shown in Figures 18 through 25. Generally, the contours showed high temperature and pressure within the vicinity of AP-2D and AP-1D, and lower values to the south. The values to the north can only be validated by drilling in that area.

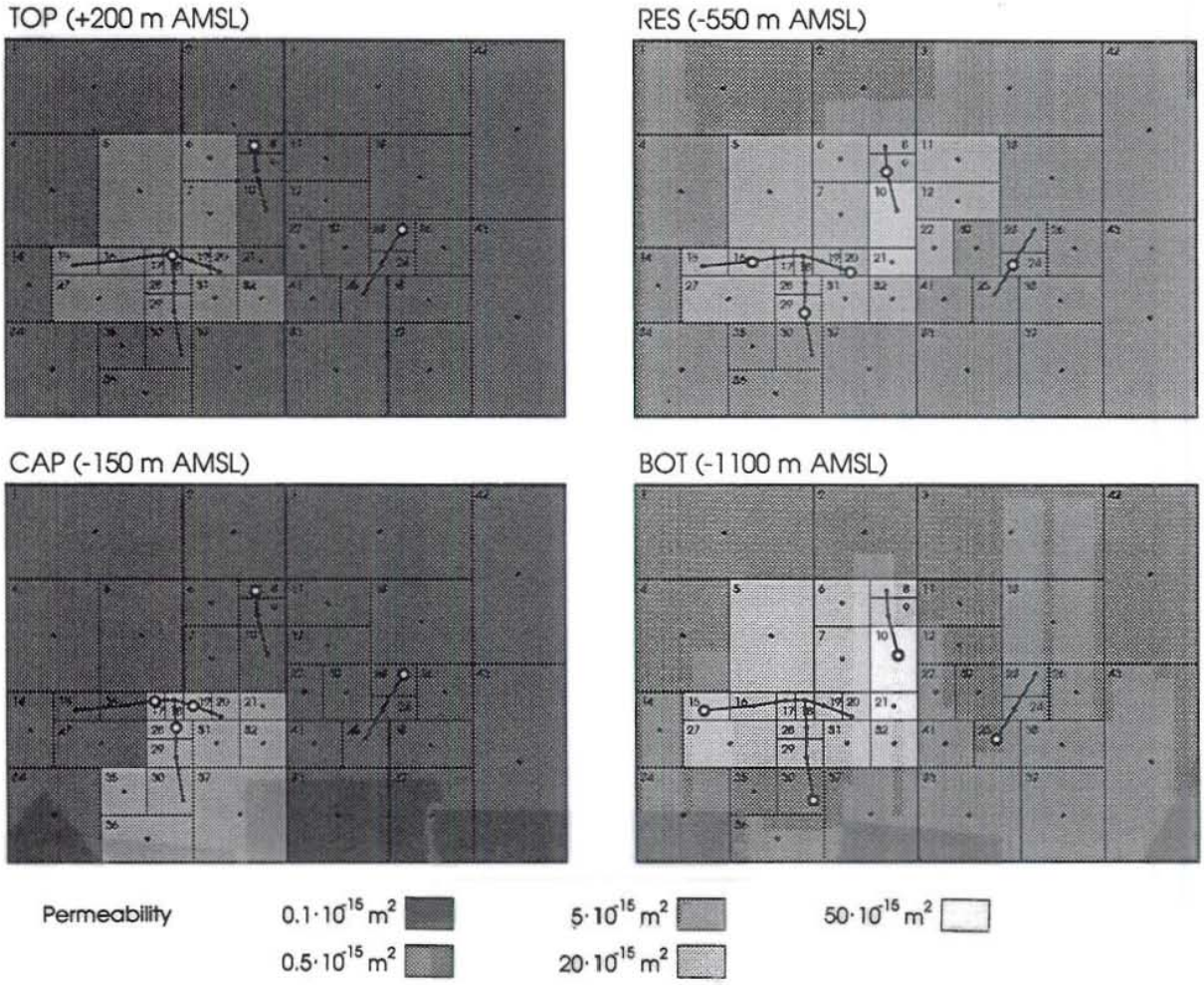

FIGURE 17: The permeability distribution in the four layers of the best-fit model

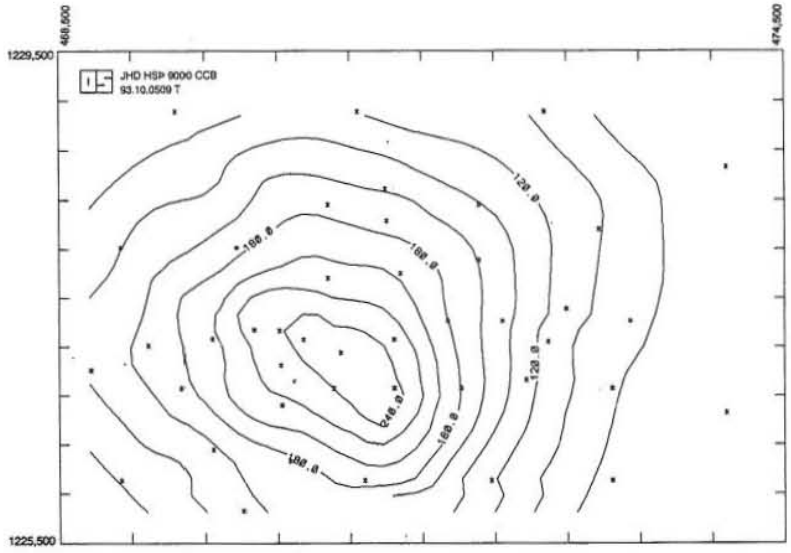

FIGURE 18: Temperature distribution in layer TOP (+200 m a.m.s.l.)

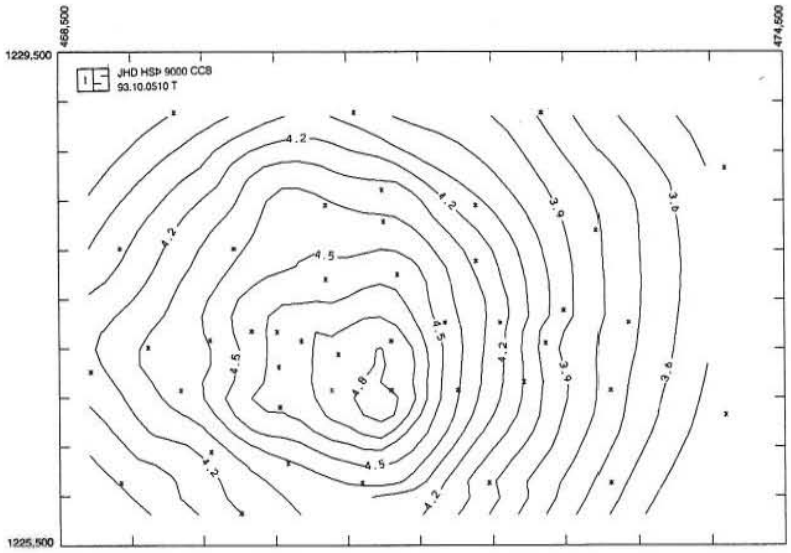

FIGURE 19: Pressure distribution in layer TOP

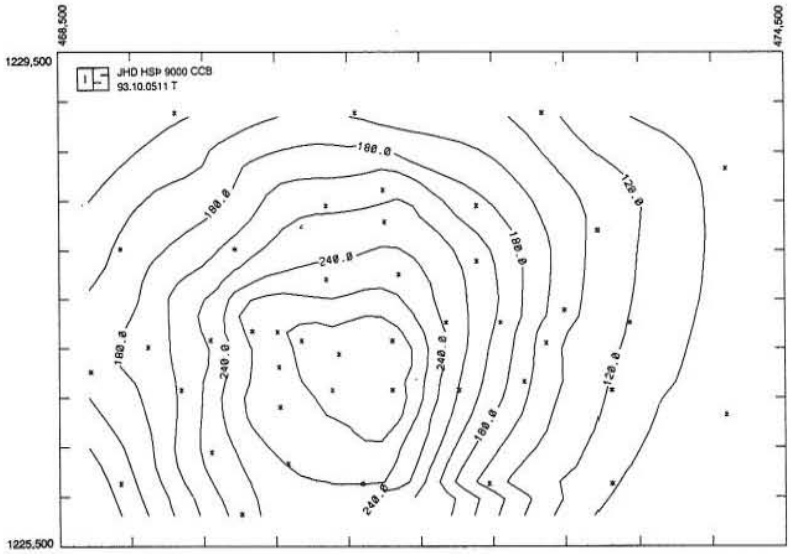

FIGURE 20: Temperature distribution in layer CAP (-150 m a.m.s.l.)

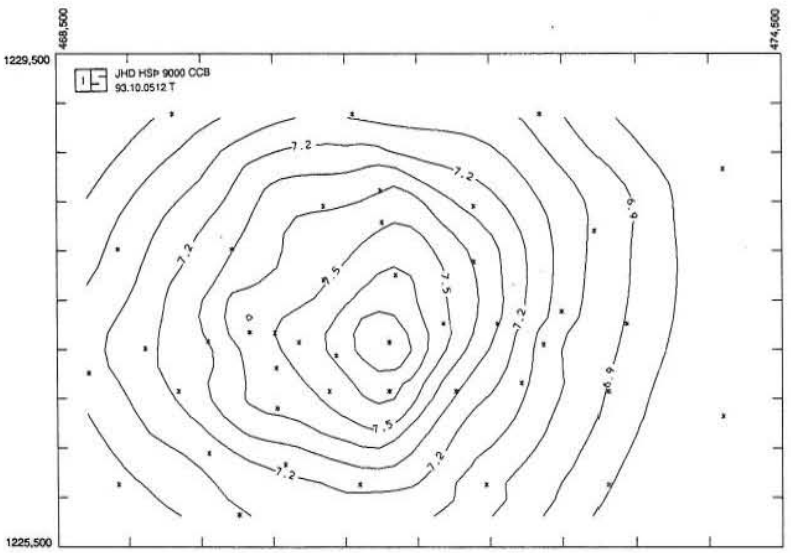

FIGURE 21: Pressure distribution in layer CAP

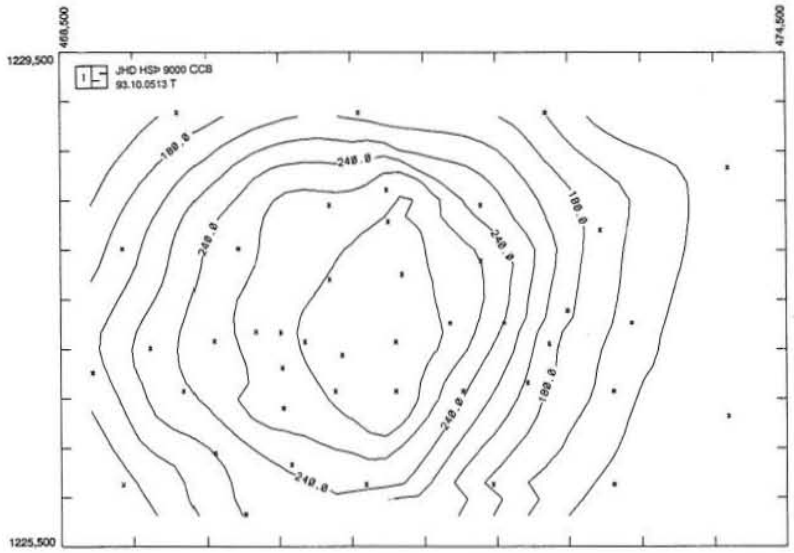

FIGURE 22: Temperature distribution in layer RES (-550 m a.m.s.l.)

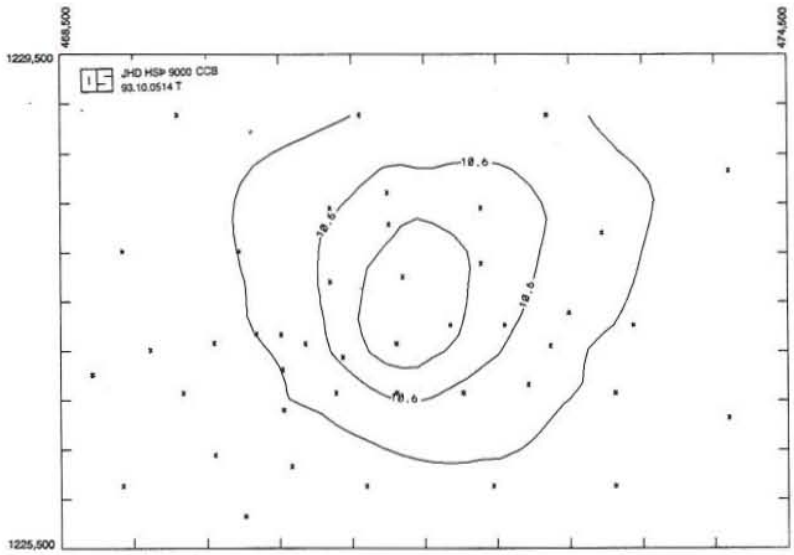

FIGURE 23: Pressure distribution in layer RES

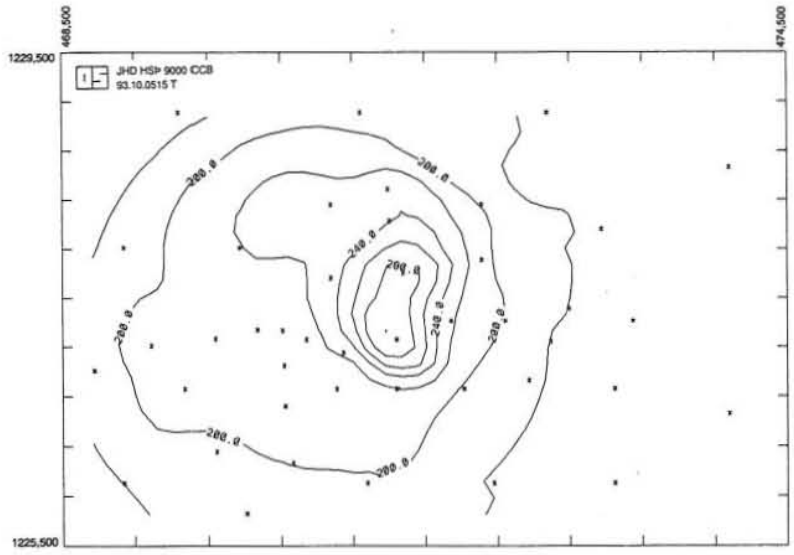

FIGURE 24: Temperature distribution in layer BOT (-1100 m a.m.s.l.)

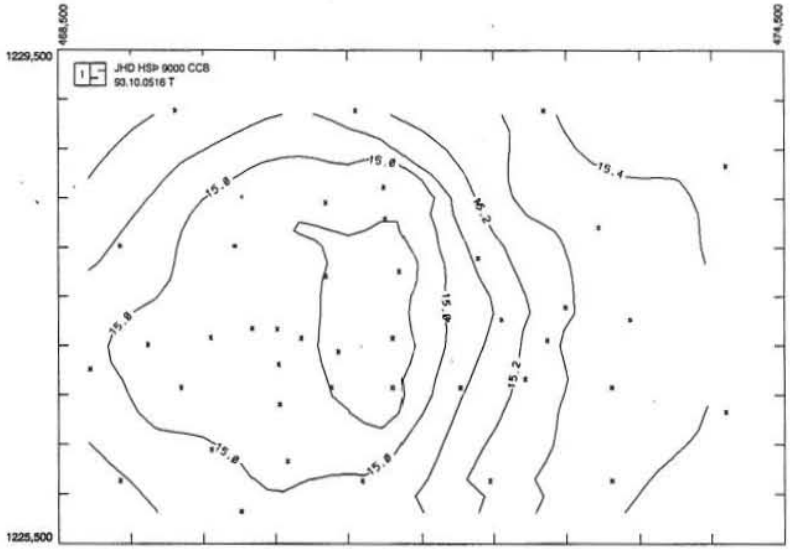

FIGURE 25: Pressure distribution in layer BOT

6. CONCLUSIONS AND RECOMMENDATIONS

The natural state simulation study done on the Alto Peak geothermal field using the software TOUGH was able to replicate the temperature and pressure distribution in the field, especially the thermal inversion in the lower zones of AP-1D, AP-4D and AP-5D. The resulting permeability distribution from the temperature and pressure match between the estimated stable formation values and the simulated data ranged from 0.1 to 50.0 mD.

This model, however, should further be refined and adjusted for it to eventually serve as basis for creating an exploitation model, whereby production data is assimilated into the analysis. In this case, storage parameters will be calibrated against production data. A possible improvement to the model is the representation of the apparent leakage in the upper zone of AP-2D in the three-dimensional grid.

ACKNOWLEDGEMENTS

I would like to express my gratitude to all the special people that have made this UNU Fellowship a most welcome learning opportunity for me, as well as a great privilege on my part for having had the chance to work closely with them:

- Dr. Ingvar Birgir Fridleifsson for his unqualified support and unwavering enthusiasm for the welfare of the UNU Fellows, likewise to Ludvik Georgsson and Margret Westlund for the countless things they did for us;

- the Orkustofnun family for their friendly assistance, especially to Helga and Audur for the drawings that complemented this report;

- the geothermal course lecturers and the Reservoir Engineering staff for their inspired teaching and guidance;

- the UNU fellows, especially to my good friends Noel, Manuel, Vlady and Hu for all the sharing and the learning;

- and my adviser, Dr. Pordur Arason, simply for everything.

Finally, thank you to my beloved family and to my dear friends in PNOC (Cris, Malou and Do) for all the happiness and inspiration you have given me. Thank you for seeing me through.

REFERENCES

Bodvarsson, G.S., Pruess, K., and Lippmann, M.J., 1986: Modelling of geothermal systems. Journal of Petroleum Technology, Society of Petroleum Engineers, 1007-1021.

Bodvarsson, G.S., and Witherspoon, P.A., 1989: Geothermal reservoir engineering. Geothermal Science and Technology, Vol. 2, Part 1, 1-68.

O'Sullivan, M.J., and McKibbin, R., 1989: Geothermal reservoir engineering. Geothermal Institute, University of Auckland, 174 pp.

Pruess, K., 1987: TOUGH user's guide. Lawrence Berkeley Laboratory, University of California, Berkeley, 78 pp.

Reyes, A.G., Salera, J.R.M.S., Rodis, N.O., Sanchez, D.R., Vergara, M.C., Ogena, M.S., Bayrante, L.F., Catane, J.P.L., Herras, E.B., Maneja, F.C., Pagado, E.S., Ramos, M.N., and Salonga, N.D., 1992: Post-drilling geoscientific evaluation of the Alto Peak geothermal system, Leyte. PNOC-EDC, internal report, Manila, 129 pp.

Salonga, N.D., Salera, J.R.M.S., Clemente, V.C., Vergara, M.C., Bayon, F.E.B., Urmeneta, N.N.A., and Delfin, M.C.Z., 1993: Alto Peak geothermal field, resource assessment update. PNOC-EDC, internal report, Manila, 164 pp.